Fruit Research

ARTICLE

Open Access

https://doi.org/10.48130/FruRes-2022-0012

Fruit Research **2022**, 2:12

Extreme-phenotype GWAS unravels a complex nexus between apple (*Malus domestica*) red-flesh colour and internal flesh browning

Satish Kumar[1*], Cecilia H. Deng[2], Claire Molloy[1], Chris Kirk[3], Blue Plunkett[2], Kui Lin-Wang[2], Andrew Allan[2], and Richard Espley[2]

[1] *The New Zealand Institute for Plant and Food Research Limited, Hawke's Bay Research Centre, Havelock North 4130, New Zealand*
[2] *The New Zealand Institute for Plant and Food Research Limited, Mount Albert Research Centre, Auckland 1025 , New Zealand*
[3] *The New Zealand Institute for Plant and Food Research Limited, Palmerston North Research Centre, Palmerston North 4410, New Zealand*
* Corresponding author, E-mail: Satish.Kumar@plantandfood.co.nz

Abstract

The genetic link between apple red flesh (RF) coloration and the internal flesh browning disorder (FBD) is a major challenge when breeding high fruit quality RF apple cultivars. A genome-wide association study (GWAS) was conducted in a population of about 900 red-leaved seedlings to identify genomic regions and putative candidate genes using whole genome sequencing of the pools of extreme phenotypes (XP) for the RF colour coverage (using the weighted cortex index (WCI)) and FBD. This study identified novel genomic regions contributing to WCI and FBD variation in the red-leaved seedlings. The FBD-associated regions were enriched for genes regulating senescence, heat shock proteins, cytochrome P450, ascorbate metabolism and pectin methyl esterases. Although there were no significant regions in common for WCI and FBD, there were several genes (e.g. MYB85, MYB66, ethylene insensitive 3, DNAJ heat shock protein, WRKY7, and NAC42) enriched commonly between the genomic regions associated with these traits, potentially underpinning the genetic connection between WCI and FBD. Some of the differentially expressed genes between the R6:MdMYB10 and white-fleshed 'control' apples resided within the GWAS hotspot for WCI (e.g. chalcone synthase, UDP-Glycosyl transferase) and FBD (e.g. Rho GTPase activating protein, lipoxygenase 1, phytoene synthase) – validating the XP-GWAS findings. Paralogs of several genes resided in the trait-associated genomic regions, suggesting that whole genome duplication plays an important role in the regulation of these traits. Adverse genetic correlations between WCI and sensory traits were observed, and strategies to develop FBD-free high fruit quality RF cultivars are discussed.

Citation: Kumar S, Deng C, Molloy C, Kirk C, Plunkett B, et al. 2022. Extreme-phenotype GWAS unravels a complex nexus between apple (*Malus domestica*) red-flesh colour and internal flesh browning. *Fruit Research* 2:12 https://doi.org/10.48130/FruRes-2022-0012

INTRODUCTION

The competition for consumer preference for fresh apples (*Malus domestica*) from exotic and tropical fruits is intense. Red-fleshed (RF) apple may not only provide a novel point of differentiation and enhanced visual quality, but also a source of increased concentration of potentially health-benefiting compounds within both the fresh fruit and snack/juice markets[1]. Two different types of RF apples have been characterised: Type 1 RF apple has red colouration not only in the fruit core and cortex, but also in vegetative tissues, including stems and leaves; Type 2 RF apples display red pigment only in the fruit cortex[1,2]. To facilitate trade and lengthen the supply-window, harvested fruit are usually cold stored, which can induce a series of disorders, including physiological breakdown manifesting as a flesh browning disorder (FBD) in RF apples[3,4]. FBD in RF apples can be caused by senescence, and there is also some evidence to suggest that a large proportion of RF apples are chilling-sensitive (Jason Johnston, Plant & Food Research Hawke's Bay, *personal communication*).

Earlier studies suggested that Type 1 RF colour was determined by a promoter mutation of *MdMYB10* that has a tandem replication of a myeloblastosis (MYB) binding *cis*-element (R6) within the promoter, resulting in autoregulation of *MdMYB10*[5]. However, van Nocker et al.[6] observed a large variation in the degree and pattern of red pigmentation within the cortex among the accessions carrying *MdMYB10*, and concluded that the presence of this gene alone was not sufficient to ensure the RF colour. A genome-wide association study (GWAS)[3], reported that, in addition to the *MdMYB10* gene, other genetic factors (e.g. *MdLAR1*, a key enzyme in the flavonoid biosynthetic pathway) were associated with RF colour, too. Wang et al.[7] reported that many of the up-regulated genes in RF apples were associated with flavonoid biosynthesis (e.g., chalcone synthase (CHS), chalcone isomerase (CHI), dihydroflavonol 4-reductase (DFR), anthocyanin synthase (ANS), UDP-glucosyl-transferase (UGT) and MYB transcription factors). Recently, *MdNAC42* was shown to share similar expression patterns in RF fruit with *MdMYB10* and *MdTTG1*, and it interacts with *MdMYB10* to participate in the regulation of anthocyanin synthesis in the RF apple Redlove®[8].

Several transcription factor genes (e.g., MYB, WRKY, bHLH, NAC, ERF, bZIP and HSF) were reported to be differentially expressed during cold-induced morphological and physiological changes in 'Golden Delicious' apples[9]. A study by Zhang et al.[10] showed that ERF1B was capable of interacting with the promotors of anthocyanin and proanthocyanidin (PA) MYB transcription factors, and suggested that ethylene regulation and anthocyanin regulation might be linked in either direction. It was reported that ethylene signal transduction pathway

genes or response genes, such as ERS (ethylene response sensor), EIN3 (ethylene-insensitive3) and ERFs (ethylene response factors), may play an important role in the regulatory network of PA biosynthesis[11].

Espley et al.[12] observed no incidence of FBD in cold-stored fruit of 'Royal Gala', but over-expression of *MdMYB10* in 'Royal Gala' resulted in a high rate of FBD in RF fruit, which was hypothesised to be caused by elevated fruit ethylene concentrations before harvest and more anthocyanin, chlorogenic acid (CGA) and pro-cyanidins in RF fruit. In addition, the MYB10 transcription factor was shown to elevate the expression levels of *MdACS*, *MdACO,* and *MdERF106* ethylene-regulating genes[12]. To elucidate the mechanism regulating the FBD of RF apples, Zuo et al.[13] analysed the transcriptome of tree-ripe apples at 0, 0.5 and 4 h after cutting, and reported that the differentially expressed genes at different sampling points were mainly related to plant–pathogen interactions.

GWAS is a powerful technique for mining novel functional variants. One of the limitations of GWAS, using SNP arrays, is that they require genotyping of large numbers of individuals, which may be expensive for large populations. DNA pooling-based designs (i.e., bulk segregant analysis) test differential allele distributions in pools of individuals that exhibit extreme phenotypes (XP) in bi-parental populations, large germplasm collections or random mating populations[14–16]. In addition to reducing the number of samples to be genotyped, the use of whole genome sequencing (WGS)-based XP-GWAS has the potential to identify small-effect loci and rare alleles via extreme phenotypic selection.

In this WGS-based XP-GWAS, we investigated the genetic basis of RF and FBD by sequencing the pools of individuals that exhibited extreme phenotypes for these two traits, and analysed the differences in allele frequencies between phenotypic classes. This method combines the simplicity of genotyping pools with superior mapping resolution. We also examined the transcriptome from transgenic apple fruit harbouring the R6:MYB10 promoter as a model for red flesh in apple. Differences in gene expression of a highly pigmented line were compared with expression in control fruit and these genes were then used for comparison with the seedling population. Understanding the genetic basis of the link between RF and FBD will help in design of strategies for selection against FBD in high-quality Type 1 RF apple cultivars.

RESULTS

Genetic parameters

A snapshot of visual variation in FBD and WCI is presented in Fig. 1. The average WCI and FBD across all ~900 seedlings ranged from 0 to 7, and from 0% to 58%, respectively. Based on the MLM analysis, the estimated narrow-sense heritability (h^2) of WCI and FBD was 0.57 (standard error = 0.18) and 0.09 (standard error = 0.05), respectively. The estimated genetic correlation between WCI and FBD was 0.58, and several fruit quality traits displayed unfavourable correlations with WCI (Supplemental Fig. S1). Seedlings with higher WCI scores were generally characterised by poor firmness and crispness, plus higher astringency and sourness. Estimated phenotypic and genetic correlations between all pairs of traits are listed in Supplemental Table S1.

Characteristics of DNA pools, and variant calling

A few seedlings had no red pigment in the cortex, but the average WCI score across all seedlings was 2.25. About two-thirds of the seedlings did not display any FBD symptoms, but among the remaining seedlings, FBD ranged between 1% and 58% (Fig. 2). The average WCI score for the 'low' and 'high' WCI pool was 0.45 and 5.2, respectively, while the average FBD was 0% and 20.6% for the 'low' and 'high' FBD pool, respectively (Supplemental Table S2). The average WCI score of the seedlings in the FBD pools was similar (Low: 5.5; High: 4.6), while the average FBD of the high- and low-WCI pools was 4.5% and 0.1%, respectively.

FBD-associated genomic regions, and candidate gene screening

After filtering, about 204,000 SNPs were used and the average sequencing depth of SNP loci was similar for the two pools (42 vs 44). There was a near-perfect correlation between the Z-test statistics and G-statistics, so only the latter are discussed hereafter. A plot of the G' values, smoothed over 2 Mb windows, is shown for all 17 chromosomes (Chrs) in Supplemental Fig. S2. XP-GWAS identified genomic regions

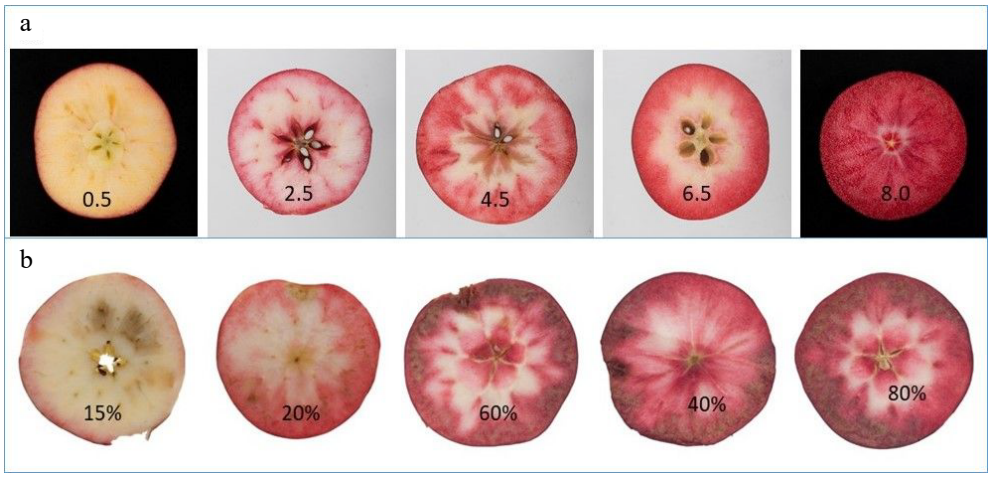

Fig. 1 Transverse cross-sections of apple slices showing range in (a) flesh colouration, and (b) flesh browning disorder for Type 1 red-fleshed apple. The weighted cortical intensity (WCI) scores (0–9 scale) and the proportion of the cortex area showing symptoms of flesh browning disorder are also displayed.

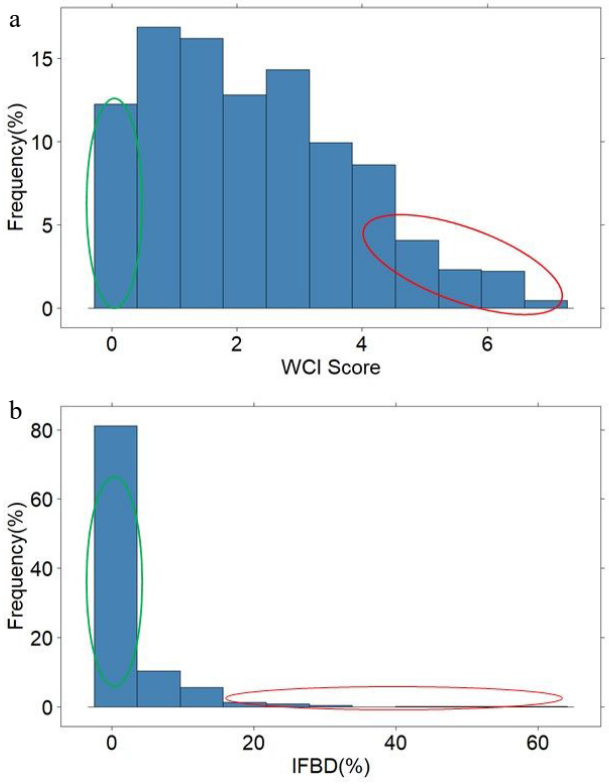

Fig. 2 The distribution of weighted cortex intensity (WCI) scores (a) and the internal flesh browning disorder IFBD%; (b) in the population of ~900 apple seedlings. The green and red circles highlight the individuals used to form the 'low' and 'high' pools of samples.

significantly associated with FBD on 12 out of the 17 Chrs (Fig. 3), and putative candidate genes within ±1.0 Mb distanceof the significant G' peaks were identified (Table 1). Additional genomic regions, which did not meet the significance threshold but displayed distinguished G' peaks, were also identified across all chromosomes (Supplemental Table S3).

The ethylene-responsive factor 13 (*MdERF13*: MD02G1213600) resided within the significant region (21.9–23.5 Mb) on Chr2, while the ascorbate peroxidase 3 (*MdAPX3*: MD02G1127800, MD02G1132200) resided in the prominent region between 9.45 and 11.28 Mb) (Fig. 3, Table 1). There were several genomic regions showing association with FBD on Chr3. The first region (8.2–9.5 Mb) flanked *MdAPX1* (MD03G1108200, MD03G1108300), while *MdERF3* (MD03G1194300) and heat shock protein 70 (HSP70: MD03G1201800, D03G1201700) resided within the prominent peak region (25.5–27.5 Mb). Another significant region (36.5–37.5 Mb) at the bottom on Chr3 harboured ethylene response sensor 1 (*MdERS1*: MD03G1292200), a flavonoid-biosynthesis related protein *MdMYB12* (MD03G1297100), HSP DnaJ and pectin methyl esterase (PME) inhibitor proteins (Fig. 3, Table 1).

The significant G' region (27.6–29.6 Mb) on Chr4 flanked the genes MD04G1188000 and MD04G1188400 involved in the biosynthesis of hydroxycinnamoyl CoA shikimate/quinate hydroxycinnamoyl transferase (HCT/HQT), while the adjacent region (22.1–24.3 Mb) harboured a cluster of UDP-glucosyl-transferase (UGT) proteins and HSP (Table 1). Another region between 11.0 and 13.0 Mb encompassed phenylalanine and lignin biosynthesis gene MYB85 (MD04G1080600)[17]. The only significant region associated with FBD on Chr6 spanned between 29.8 and 31.7 Mb, which included a SNP earlier reported associated with FBD[4]. This region also harboured

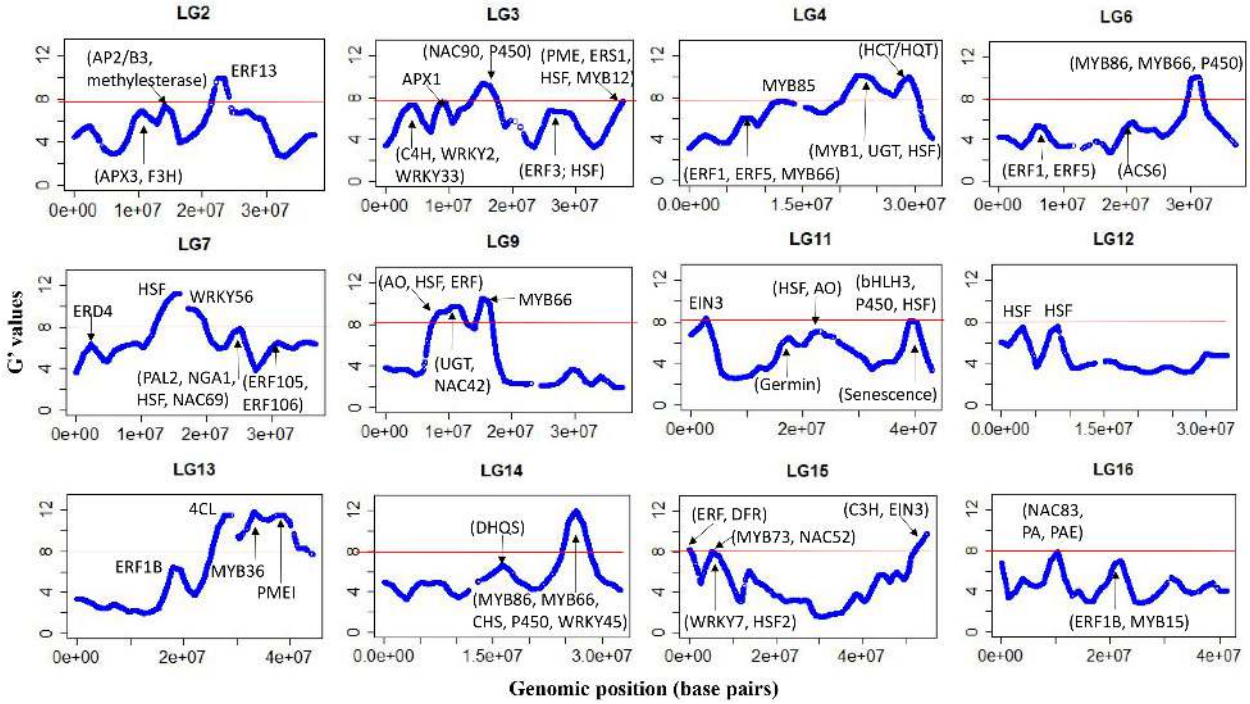

Fig. 3 G'-statistics across the linkage groups (LG) showing significant association with the flesh browning disorder (FBD) in apple The horizontal red lines indicate the significance threshold. The putative candidate genes (refer to Table 1) underpinning various G' peaks are also shown.

Table 1. A list of the genomic regions associated with internal flesh browning disorder (FBD) in apples. Putative candidate genes residing within these regions are also listed using GDDH13v1.1 reference genome assembly.

Chr	Genomic region (Mb)	Putative genes functions
2	21.9–23.5	Ethylene-responsive element binding factor 13 (MdERF13: MD02G1213600);
3	3.1–4.9	cinnamate 4-hydroxylase (C4H) enzyme (MD03G1051100, MD03G1050900 and MD03G1051000); MdWRKY2: MD03G1044400; MdWRKY33 (MD03G1057400)
3	8.2–9.6	ascorbate peroxidase 1 (MdAPX1: MD03G1108200, MD03G1108300)
3	14.7–16.6	senescence-related MdNAC90 (MD03G1148500)
3	36.5–37.5	Ethylene response sensor 1 (MdERS1: MD03G1292200); flavonoid biosynthesis protein MdMYB12 (MD03G1297100); Heat shock protein DnaJ (MD03G1296600, MD03G1297000); pectin methylesterase (MdPME) inhibitor protein (MD03G1290800, MD03G1290900, MD03G1291000).
4	11.0–13.0	phenylalanine and lignin biosynthesis protein MdMYB85 (MD04G1080600)
4	22.1–24.4	MYB domain protein 1 (MD04G1142200); HSP20-like protein (MD04G1140600); UDP-glucosyltransferase (UGT) proteins UGT85A7 (MD04G1140700, MD04G1140900); UGT85A3 (MD04G1140800); UGT (MD04G1141000, MD04G1141300); UGT85A2 (MD04G1141400); UGT85A4 (MD04G1141500); DNAJ heat shock protein (MD04G1153800, MD04G1153900, MD04G1154100)
4	27.6–29.6	HCT/HQT regulatory genes MD04G1188000 and MD04G1188400
6	29.8–31.7	Volz et al. (2013) QTL for IFBD; anthocyanin regulatory proteins MdMYB86 (MD06G1167200); triterpene biosynthesis transcription factor MdMYB66 (MD06G1174200); Cytochrome P450 (MD06G1162600; MD06G1162700, MD06G1162800, MD06G1163100, MD06G1163300, MD06G1163400, MD06G1163500, MD06G1163600, MD06G1163800, MD06G1164000, MD06G1164100, MD06G1164300, MD06G1164400, MD06G1164500, MD06G1164700)
7	13.9–15.9	heat shock protein 70B (MD07G1116300)
7	17.4–19.0	Drought-stress WRKY DNA-binding proteins (MdWRKY56: MD07G1131000, MD07G1131400)
7	23.6–25.2	MdPAL2 (MD07G1172700); drought-stress gene NGA1 (MD07G1162400); DNAJ heat shock family protein (MD07G1162300, MD07G1162200), stress-response protein (MdNAC69: MD07G1163700, MD07G1164000)
9	7.9–11.8	MD09G1110500 involved in ascorbate oxidase (AO); MdUGT proteins (MD09G1141200, MD09G1141300, MD09G1141500, MD09G1141600, MD09G1141700, MD09G1141800, MD09G1142000, MD09G1142500, MD09G1142600, MD09G1142800, MD09G1142900, MD09G1143000, MD09G1143200, MD09G1143400) involved in flavonoids biosynthesis; heat shock proteins 89.1 (MD09G1122200) and HSP70 (MD09G1137300); Ethylene-forming enzyme MD09G1114800; Anthocyanin regulatory protein MdNAC42 (MD09G1147500, MD09G1147600)
9	14.9–16.5	triterpene biosynthesis transcription factor protein MdMYB66 (MD09G1183800);
11	1.7–3.0	ethylene response factor proteins (MdEIN-like 3: MD11G1022400)
11	38.6–40.6	Senescence-related gene 1 (MD11G1271400, MD11G1272300, MD11G1272000, MD11G1272100, MD11G1272300, MD11G1272400, and MD11G1272500); Chalcone-flavanone isomerase (CHI) protein (MD11G1273600) and MdbHLH3 (MD11G1286900, MDP0000225680); cytochrome P450 enzyme (MD11G1274000, MD11G1274100, MD11G1274200, MD11G1274300, MD11G1274500, and MD11G1274600); heat shock transcription factor A6B (MdHSFA6B: MD11G1278900) – involved in ABA-mediated heat response and flavonoid biosynthesis.
12	2.2–3.5	heat shock protein 70-1 ((MD12G1025600, MD12G1025700 and MD12G1026300) and heat shock protein 70 (MD12G1025800 and MD12G1025900 and MD12G1026000); ethylene (MD12G1032000) and auxin-responsive (MD12G1027600) proteins.
12	7.2–8.4	DNAJ heat shock domain-containing protein (MD12G1065200 and MD12G1067400)
13	27.5–30.5	MD13G1257800 involved in polyphenol 4-coumarate:CoA ligase (4CL)
13	37.5–39.5	pectin methyl esterase inhibitor superfamily protein MdPMEI (MD13G1278600)
14	25.4–27.5	Drought-stress response gene MdWRKY45 (MD14G1154500); chalcone synthase (CHS) family proteins (MD14G1160800 and MD14G1160900); triterpene biosynthesis transcription factor MdMYB66 (MD14G1180700, MD14G1181000, MD14G1180900); anthocyanin biosynthesis protein (MdMYB86: MD14G1172900); cytochrome P450 proteins (MD14G1169000, MD14G1169200, MD14G1169600, MD14G1169700)
15	0–1.5	Ethylene synthesis proteins (MD15G1020100, MD15G1020300 and MD15G1020500); dihydroflavonol reductase (DFR) gene (MD15G1024100)
15	4.6–6.8	MdMYB73 (MD15G1076600, MD15G1088000) modulates malate transportation/accumulation via interaction with MdMYB1/10; MdNAC52: MD15G1079400) regulates anthocyanin/PA; heat shock transcription factor B4 (MD15G1080700); stress-response protein MdWRKY7 (MD15G1078200)
15	53.5–54.9	*MdC3H* (MD15G1436500) involved in chlorogenic acid biosynthesis; MdEIN3 (MD15G1441000) involved in regulating ethylene synthesis and anthocyanin accumulation
16	8.9–10.9	SAUR-like auxin-responsive protein (MD16G1124300) and MdNAC83: (MD16G1125800) associated with fruit ripening; MD16G1140800 regulates proanthocyanidin; MdPAE genes (MD16G1132100, MD16G1140500) regulates ethylene production.

several MYB proteins (*MdMYB86*: MD06G1167200; *MdMYB98*: MD06G1172900; *MdMYB66*: MD06G1174200) and a large cluster of cytochrome P450 proteins (Table 1).

A significant FBD-associated region (13.9–15.9 Mb) on Chr7 encompassed the HSP 70B (MD07G1116300), while another significant region between 23.6 Mb and 25.2 Mb flanked the gene coding for phenylalanine ammonia lyase 2 (*MdPAL2:* MD07G1172700), a drought stress gene NGA1 (MD07G1162400), DNAJ HSP, and stress-response protein (*MdNAC69*: MD07G1163700, MD07G1164000) (Fig. 3, Table 1). A large significant region spanning between 7.9 and 11.8 Mb on Chr9 encompassed the gene MD09G1110500 putatively involved in ascorbate oxidase (AO), HSP (HSP70: MD09G1137300; HSP89.1: MD09G1122200), an ethylene-forming enzyme (MD09G1114800), and MdNAC42 (MD09G1147500, MD09G1147600). Another significant genomic region on Chr9 was between 14.9 and 16.5 Mb, which harbours the MYB domain protein *MdMYB66* (MD09G1183800) (Table 1).

A sharp G' peak region (1.7–3.0 Mb) on Chr11 associated with FBD encompassed ethylene insensitive 3 (*MdEIN3*: MD11G1022400) along with a cluster of UGT proteins, WD-40, and bHLHL proteins (Table 1). A significant region between 38.6 and 40.6 Mb at the bottom of Chr11 was dominated by clusters of senescence-related genes and cytochrome P450 enzymes. This

genomic region also flanked a chalcone-flavanone isomerase (CHI) family protein (MD11G1273600) and a bHLH protein (*MdbHLH3*: MD11G1286900, MDP0000225680), along with the heat shock transcription factor A6B (HSFA6B: MD11G1278900) (Table 1, Supplemental Table S3).

The region (2.2–3.3 Mb) associated with FBD on Chr12 flanked genes for the HSP 70 and 70-1, NAC proteins, ethylene and auxin-responsive proteins (Table 1). An adjacent significant region (7.2–8.4 Mb) flanked DNAJ HSP, along with bZIP, bHLH and WD-40 repeat-like proteins (Table 1; Supplemental Table S3). There was a large genomic region on Chr13 showing a significant association with FBD. In this region, the first G' peak (27.5–30.5 Mb) harboured MD13G1257800, which regulates polyphenol 4-coumarate: CoA ligase (4CL) synthesis. The second G' peak region (32.6–34.7 Mb) corresponded to an earlier mapped QTL for flesh browning in white-fleshed apples[18].

The significant region (25.4–27.5 Mb) on Chr14 harboured various genes for proteins with different putative functions, such as AP2 proteins, WD-40 repeat family proteins, bHLH proteins, *MdNAC83* (MD14G1150900), *MdWRKY45* (MD14G1154500), chalcone synthase (CHS) family proteins (MD14G1160800 and MD14G1160900), cytochrome P450 proteins, and several MYB domain proteins (*MdMYB86*: MD14G1172900; *MdMYB98*: MD14G1179000; *MdMYB66*: MD14G1180700, MD14G1181000, MD14G1180900) (Fig. 3, Table 1, Supplemental Table S3). A sharp G' peak (15.2–17.2 Mb) on Chr14 did not meet the significance threshold corresponding to the FBD QTL in white-fleshed apples[18].

The upper 1.5 Mb region on Chr15 associated with FBD encompassed several transcription factor families, including WD-40 repeats, bHLH, bZIP, ethylene synthesis proteins, and dihydroflavonol reductase (DFR) protein (MD15G1024100) (Fig. 3, Table 1; Supplemental Table S3). Another significant region on Chr15 (4.6–6.8 Mb) harboured HSF B4, *MdMYB73* (which interacts with *MdMYB1/10* to modulate malate transportation) and *MdNAC52* (MD15G1079400), which regulates anthocyanin and PA synthesis by directly regulating *MdLAR*[19]. A significantly associated region at the bottom of Chr15 (53.5–54.9 Mb) harboured *MdNAC35* (MD15G1444700), *MdC3H* (MD15G1436500) involved in the production of p-coumarate 3-hydroxylase (C3H) enzyme, which plays a role in chlorogenic acid biosynthesis, and *MdEIN3* (MD15G1441000).

The significant region between 8.9 and 10.9 Mb on Chr16 harboured a gene for SAUR-like auxin-responsive protein (MD16G1124300) and *MdNAC83* (MD16G1125800), both of which have been reportedly associated with apple fruit ripening[20]. This region also encompassed MD16G1140800, which regulates PA[11], and a gene for the pectin acetyl esterase protein *MdPAE10* (MD16G1132100) involved in ethylene production and shelf-life[21]. A sharp G' peak region (20.4–22.4 Mb) in the middle of Chr16 flanked *MdERF1B* (MD16G1216900) and *MdMYB15* (MD16G1218000 and MD16G1218900), involved in altering anthocyanin and PA concentrations[10] (Fig. 3, Table 1, Supplemental Table S3).

WCI-associated genomic regions, and candidate genes screening

The average sequencing depth of the SNP loci (~160,000) retained for marker-trait association was similar for the two WCI pools (41 vs 44). The significant regions were located on Chrs 2, 4, 6, 7, 10, 15 and 16 (Fig. 4). The genomic intervals within ±1.0 Mb of the significant G' peaks, and the putative candidate genes within those intervals, are listed in Table 2. Additional genomic regions, which did not meet the significance threshold but displayed distinct G' peaks, were also identified across most chromosomes (Supplemental Fig. S2, Supplemental Table S3). A significant region on Chr4 encompassed chalcone synthase (CHS) genes, along with an ERF (MD04G1009000) involved in regulating PA biosynthesis[11].

There were distinct G' peaks within a large genomic region (spanning between 9.0 and 18.0 Mb) significantly associated with WCI on Chr6 (Fig. 4). The G' peak region 12.1–13.6 Mb encompassed *MdMYB85* (MD06G1064300), and a gene for a pectin methyl esterase

(PME) inhibitor protein (MD06G1064700); while the region between 16.0 and 17.6 Mb flanked the genes involved in leucoanthocyanidin dioxygenase (LDOX) synthesis (Table 2). The auxin response factor 9 (*MdARF9*: MD06G1111100) and the HSP70 (MD06G1113000) resided in the significant region between 24.0 and 26.0 Mb on Chr6 (Table 2).

The genomic region (4.1–5.6 Mb) with significant association with WCI on Chr7 flanked *MdEIN3* (MD07G1053500, MD07G1053800), which plays an important role in the regulatory network of PA biosynthesis[11]. A significant region (35.6–38.7 Mb) on Chr10 encompassed gene clusters for bHLH and WRKY proteins along with an ethylene repressor factor (*MdERF2*: MD10G1286300) (Fig. 4, Table 2; Supplemental Table S3). This region also harboured *MdERF4* (MD10G1290400), *MdERF12* (MD10G1290900) and NAC domain genes (*MdNAC73*: MD10G1288300), which have been reported to be associated with fruit ripening[20]. In addition, there was a cluster of polyphenol oxidase (PPO) genes residing in this region (Table 2).

On Chr15, the significant WCI-associated region spanning between 31.7 Mb and 34.2 Mb encompassed several TF families, including *MdMYB93* (MD15G1323500) (Fig. 4, Table 2, Supplemental Table S3). A distinguished G' peak region (24.9–26.9 Mb) on Chr15 harboured genes for WD-40 repeat-like proteins, bHLH proteins, redox responsive transcription factor 1 (MD15G1283200), cytochrome P450 proteins, HSF4 (MD15G1283700), and *MdWRKY7* (MD15G1287300). The *MdMYB73* (MD15G1288600) residing in this region has been shown to interact with *MdMYB1/10* and regulates several functions, including cold-stress response, ubiquitination and malate synthesis[22,23].

The significant 1.5–3.4 Mb region on Chr16 flanked an anthocyanin repressor MYB protein (MD16G1029400), senescence-associated gene 12 (MD16G1031600), malate transporter *MdMa2* (MD16G1045000: MDP0000244249), and two ethylene response factor genes (*MdERF118*: MD16G1043500; *MdRAV1*: MD16G1047700), which interact in retaining flesh firmness[24]. The *MdMYB62* (MD16G1040800) gene residing in this region is phylogenetically linked to *MdMYB8* (MD06G1217200), which plays a major role in flavonoid biosynthesis[25]. Another significant region (5.4–7.4 Mb) on Chr16 harboured several bHLH genes, including *MdMYB88* (MD16G1076100) involved in phenylpropanoid synthesis resulting in drought resistance[26] and ABA-mediated anthocyanin production[27]. The *MdMYB66* (MD16G1093200) gene, which is involved in triterpene biosynthesis, and the *MdWRKY72* (MD16G1077700) gene involved in anthocyanin synthesis, were also present in this region (Table 2, Fig. 4).

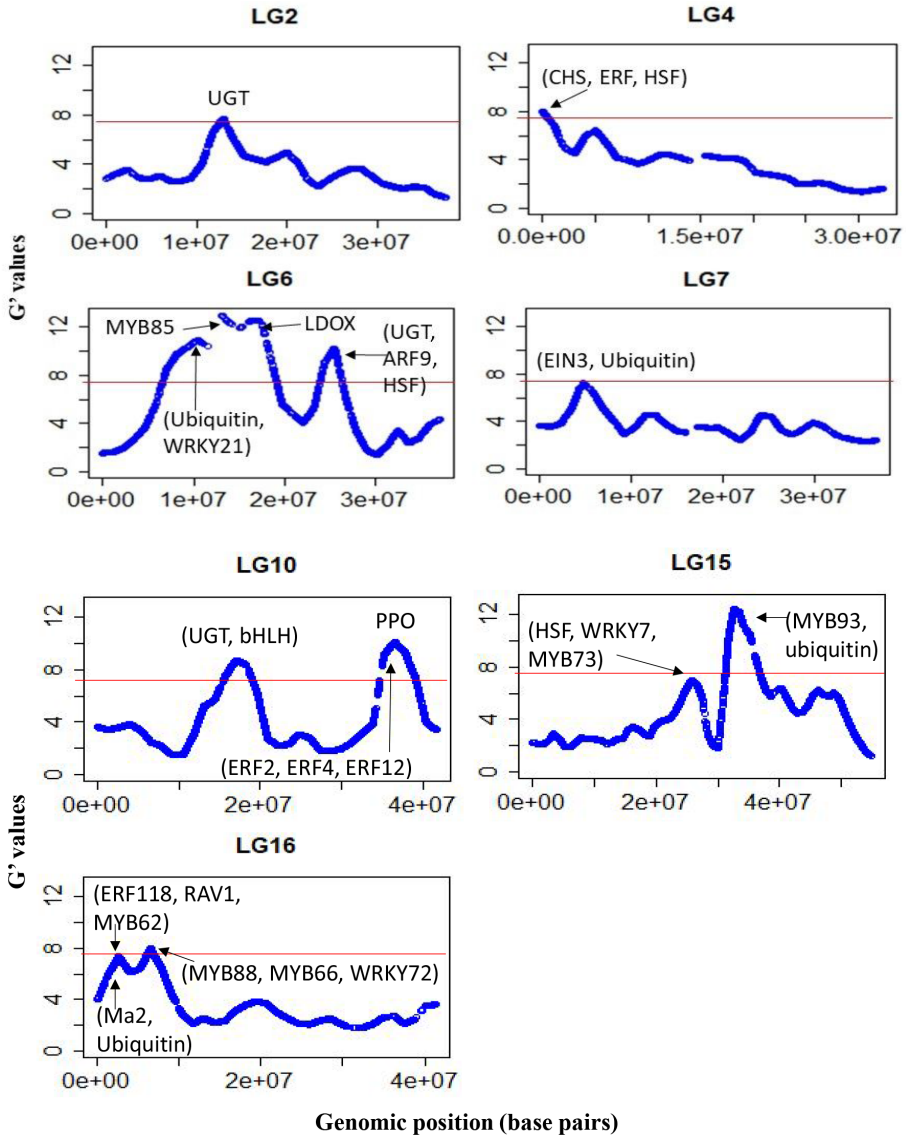

Fig. 4 G'-statistics across the linkage groups (LG) showing significant association with the weighted cortex intensity (WCI) in apple. The horizontal red lines indicate the significance threshold. The putative candidate genes (refer to Table 2) underpinning various G' peaks are also shown.

Homologous regions associated with FBD and WCI

The genomic regions tagged by XP-GWAS were enriched for regulatory functions, and several of these have a paralog (Table 3). For example, paralogues for a trio of genes (*MdMYB86*, *MdMYB98* and Cytochrome 450) resided in the FBD-associated genomic regions on Chr6 and Chr14. Several pairs of genes resided together in the FBD-associated paralog regions; for example, MdNAC90 and germin-like protein 10 on Chr3 and Chr11; WRKY55 and WRKY70 on Chr1 and Chr7; and ERF1 and ERF5 on Chr4 and Chr6. The ethylene response factor *MdERF1B* had a paralog in the FBD-associated region on Chr13 and Chr16. Interestingly, three copies of *MdNAC83* (Chrs 14, 16 17) and four copies of *MdMYB66* (Chrs 4, 6, 9 and 14) resided in the FBD-associated regions. A pair of genes (RAV1 and MYB62) resided together in the WCI-associated paralog regions on Chrs13 and 16 (Table 3).

Paralogs of several regulatory functions were also found in the regions associated with either FBD or WCI; for example, a significant region (7.9–11.8 Mb) harbouring a gene trio (*MdNAC42*, HSP70 and HSP89.1) on Chr9 was associated with FBD, but the paralogs of this trio also resided in a distinct G' region associated with WCI on Chr17 (Table 3, Supplemental Table S3). Some other examples included *MdMYB85* (Chr4 for FBD, and Chr6 for WCI), *MdEBF1* (Chr8 for WCI, and Chr15 for FBD), *MdEIN3* (Chr8 for WCI, and Chr15 for FBD), and EIN3 (Chr7 for WCI, and Chr11 for FBD). A pair of genes (*MdMYB73* and *MdWRKY7*) resided together in the separate regions associated with FBD (4.6–6.8 Mb) and WCI (24.8–26.8 Mb) within Chr15 (Table 3).

Differentially expressed genes in R6:*MdMYB10* apple fruit

The red pigmentation in fruit flesh differed amongst transgenic lines, with fruit from line A10 presenting the most deeply pigmented tissues (Supplemental Fig. S3), while those from lines A2 and A4 were similar in having a lower intensity of pigmentation. No pigmentation was observed in the flesh of

Table 2. A list of the genomic regions significantly associated with the weighted cortex intensity (WCI) in apples. Putative candidate genes residing within these regions are also listed using GDDH13v1.1 reference genome assembly.

Chr	Genomic region (Mb)	Putative genes functions
2	11.2–13.2	UDP-glucosyltransferase (UGT) proteins (MD02G1153000, MD02G1153100, MD02G1153200, MD02G1153300; MD02G1153400; MD02G1153500; MD02G1153700; MD02G1153800; MD02G1153900);
4	0–1.2	Chalcone synthase (CHS) genes (MD04G1003000; MD04G1003300 and MD04G1003400); DNAJ heat shock protein (MD04G1003500); MdERF (MD04G1009000) involved in regulating PA biosynthesis.
6	9.5–11.0	Ubiquitin protein (MD06G1061100); stress-response WRKY protein MdWRKY21 (MD06G1062800);
6	12.1–13.6	pectin methylesterase inhibitor superfamily protein (MdPME: MD06G1064700); phenylalanine and lignin biosynthesis gene (MdMYB85)
6	16.0–17.6	MD06G1071600 (MDP0000360447) involved in leucoanthocyanidin dioxygenase (LDOX) synthesis
6	24.0–26.0	UDP-glycosyltransferase proteins (MD06G1103300, MD06G1103400, MD06G1103500 and MD06G1103600); auxin response factor 9 (MdARF9: MD06G1111100) and heat shock protein 70 (Hsp 70; MD06G1113000).
7	4.1–5.6	Ethylene insensitive 3 protein (MdEIN3: MD07G1053500 and MD07G1053800) involved in proanthocyanidins (PA) biosynthesis; ubiquitin-specific protease (MD07G1051000, MD07G1051100, MD07G1051200, MD07G1051500, MD07G1051300, MD07G1051700 and MD07G1051800).
10	15.9–18.3	bHLH proteins (MD10G1098900, MD10G1104300, and MD10G1104600); UGT protein (MD10G1101200); UGT 74D1 (MD10G1110800), UGT 74F1 (MD10G1111100), UGT 74F2 (MD10G1111000).
10	35.6–38.6	Stress-response WRKY proteins (MdWRKY28: MD10G1266400; MdWRKY65: MD10G1275800). ethylene responsive factors (MdERF2: MD10G1286300; MdERF4: MD10G1290400, and MdERF12: MD10G1290900) and a NAC domain protein (MdNAC73: MD10G1288300); polyphenol oxidase (PPO) genes ((MD10G1298200; MD10G1298300; MD10G1298400; MD10G1298500; MD10G1298700; MD10G1299100; MD10G1299300; MD10G1299400).
15	24.8–26.8	heat shock factor 4 (MD15G1283700), drought-stress response WRKY protein 7 (MdWRKY7: MD15G1287300), MdMYB73 (MD15G1288600) involved in ubiquitination and malate synthesis
15	31.7–34.2	MYB domain protein 93 (MdMYB93: MD15G1323500) regulates flavonoids and suberin accumulation (Legay et al. 2016); ubiquitin -specific protease 3 (MD15G1318500),
16	1.5–3.4	MYB domain proteins (MD16G1029400) regulates anthocyanin; senescence-associated gene 12 (MD16G1031600); ethylene response factor proteins (MdERF118: MD16G1043500, and MD16G1047700 (*MdRAV1*); MdMYB62 (MD16G1040800) flavonol regulation; malate transporter MdMa2 (MD16G1045000: MDP0000244249), Ubiquitin-like superfamily protein (MD16G1036000),
16	5.4–7.4	MdMYB88 (MD16G1076100) regulates phenylpropanoid synthesis and ABA-mediated anthocyanin biosynthesis; MdMYB66 (MD16G1093200) regulates triterpene biosynthesis, MdWRKY72 (MD16G1077700) mediates ultraviolet B-induced anthocyanin synthesis.

control 'Royal Gala' (RG) fruit. RNAseq analysis of a representative transgenic line (A2) compared with RG revealed that a total of 1,379 genes were differentially expressed (log 2-fold), with 658 genes upregulated and 721 genes downregulated. This list was then assessed for commonality with the genomic regions and candidate genes from the XP-GWAS.

Genes that contained mis-sense SNPs (which would result in a change in predicted protein) and that were also differentially expressed between A2 red-fleshed transgenic line and white-fleshed 'Royal Gala' (control) apples included anthocyanin-related flavanone 3-hydroxylase, chalcone synthase and dihydroflavonol 4-reductase (Table 2 & 4). Many more upstream DNA variants (e.g. in potential promoter-controlling elements) were seen in this group of differentially expressed genes (DEGs) that were also in regions underlying WCI or FBD. Genes encoding enzymes that may be involved in FBD, such as a Rho GTPase activating protein, peroxidase, lipoxygenase 1, and ethylene-forming enzyme (ACO4), were DEGs and showed mis-sense SNPs, including a potential stop codon in the Rho GTPase-activating protein (Table 4). This intersection between DNA change and differential expression warrants further research to evaluate the functions of these genes.

DISCUSSION

Apple Type 1 red flesh is a complex trait influenced by interplay between several TF families

Several gene families (e.g. chalcone synthase, UGT, anthocyanin synthase, HSP, PAL, ERF, WRKY proteins, ABA, and bZIP transcription factors) residing in WCI-associated genomic regions have been reported to be associated with RF in apple[7,12,28]. Several of these genes are implicated in stress responses, suggesting that flavonoids and anthocyanin biosynthesis could also be associated with stress (e.g., drought, water loss) tolerance of RF apples[7].

MdMYB73, which may play a role in the cold-stress response[23,29], resided in the WCI-associated regions. Ethylene is among the various modulators of environmental stresses induced by factors such as drought and cold temperatures[9,28]. Several ERF proteins (e.g. *MdERF1B*, *MdERF3*) interact with the promoters of MYB domain proteins to regulate anthocyanin and proanthocyanidin (PA) accumulation in apple[10,11,30]. The WCI-associated genomic regions in our study flanked several ERFs previously reported to have roles in anthocyanin and PA regulation. *MdERF4* (MD10G1290400), one of the three ERFs residing in the WCI-associated region on Chr10, has high phylogenetic similarity with *MdERF38*, which interacts with *MdMYB1* to regulate drought-related anthocyanin biosynthesis[31]. Some ERFs (e.g. *MdERF2*: MD10G1286300; *MdERF4*: MD10G1290400, and *MdERF12*: MD10G1290900) and *MdNAC73* residing in the WCI-associated regions have been reported to be associated with fruit maturation[20] – suggesting an interaction between ethylene production and RF colour[12].

The WCI-associated region on Chr15 included a gene *MdMYB73* (MD15G1288600) involved in malate acid synthesis. Previous studies have reported that MdMYB1 regulates both anthocyanin and malate accumulation, and perhaps MdBT2 regulates *MdMYB73*-mediated anthocyanin accumulation[22,23]. The malate transporter gene *MdMa2* and the *MdMYB7* gene, involved in the regulation of anthocyanin and flavanols in RF apple[32], resided together in the WCI-associated upper region of LG16. Taken together, these results support the hypothesis that there is interplay between anthocyanin and malate accumulation in the RF apple. There was a cluster of ubiquitin-

Table 3. A list of homologues genes/genomic regions associated with the internal flesh browning disorder (IFBD) and red flesh (WCI) in apples. Putative candidate genes residing within these regions are also listed using GDDH13v1.1 reference genome assembly.

Trait	Chr (genomic region: Mb)	Gene name	Predicted gene ID	Putative function
IFBD	Chr6 (29.8–31.7 Mb)	MdMYB66	MD06G1174200	Suberin/triterpene deposition
IFBD	Chr14 (25.4–27.5 Mb)	MdMYB66	MD14G1180700, MD14G1181000, MD14G1180900	Suberin/triterpene deposition
IFBD	Chr4 (7.0–8.1 Mb)	MdMYB66	MD04G1060200	Suberin/triterpene deposition
IFBD	Chr9 (14.9–16.5 Mb)	MdMYB66	MD09G1183800	Suberin/triterpene deposition
IFBD	Chr6 (29.8–31.7 Mb)	MdMYB86	MD06G1167200	Anthocyanin regulation
IFBD	Chr14 (25.4–27.5 Mb)	MdMYB86	MD14G1172900	Anthocyanin regulation
IFBD	Chr6 (29.8–31.7 Mb)	MdMYB98	MD06G1172900	Drought stress response
IFBD	Chr14 (25.4–27.5 Mb)	MdMYB98	MD14G1179000	Drought stress response
IFBD	Chr6 (29.8–31.7 Mb)	Cytochrome P450	MD06G1162600, MD06G1162700, MD06G1162800, MD06G1163100, MD06G1163300, MD06G1163400, MD06G1163500, MD06G1163600, MD06G1163800, MD06G1164000, MD06G1164100, MD06G1164300, MD06G1164400, MD06G1164500, MD06G1164700	Flavonoid and triterpenic metabolism
IFBD	Chr14 (25.4–27.5 Mb)	Cytochrome P450	MD14G1169000, MD14G1169200, MD14G1169600, MD14G1169700	Flavonoid and triterpenic metabolism
IFBD	Chr3 (14.7–16.6 Mb)	MdNAC90	MD03G1148500	Senescence-related
IFBD	Chr11 (16.5–18.5 Mb)	MdNAC90	MD11G11679000	Senescence-related
IFBD	Chr14 (25.4–27.5 Mb)	MdNAC83	MD14G1150900	Senescence/ripening-related
IFBD	Chr16 (8.9–10.9 Mb)	MdNAC83	MD16G1125800	Senescence/ripening-related
IFBD	Chr17 (0–0. 7 Mb)	MdNAC83	MD17G1010300	Senescence/ripening-related
IFBD	Chr3 (14.7–16.6 Mb)	Germin-like protein 10	MD03G1148000	Polyphenol oxidase
IFBD	Chr11 (16.5–18.5 Mb)	Germin-like protein 10	MD11G1167000, MD11G1167100, MD11G1167400, MD11G1169200	Polyphenol oxidase
IFBD	Chr1 (26.9–28.5 Mb)	MdWRKY55	MD01G1168500	Drought stress response
IFBD	Chr7 (30.3–31.9 Mb)	MdWRKY55	MD07G1234600	Drought stress response
IFBD	Chr1 (26.9–28.5 Mb)	MdWRKY70	MD01G1168600	Drought stress response
IFBD	Chr7 (30.3–31.9 Mb)	MdWRKY70	MD07G1234700	Drought stress response
IFBD	Chr4 (7.0–8.1 Mb)	MdERF1	MD04G1058000	Ethylene responsive factor
IFBD	Chr6 (5.5–7.3 Mb)	MdERF1	MD06G1051800	Ethylene responsive factor
IFBD	Chr4 (7.0–8.1 Mb)	MdERF5	MD04G1058200	Ethylene responsive factor
IFBD	Chr6 (5.5–7.3 Mb)	MdERF5	MD06G1051900	Ethylene responsive factor
IFBD	Chr13 (18.0–20.0 Mb)	MdERF1B	MD13G1213100	Ethylene response factor 1
IFBD	Chr16 (20.4–22.4 Mb)	MdERF1B	MD16G1216900	Ethylene response factor 1
WCI	Chr13 (2.6–4.4 Mb)	*MdRAV1*	MD13G1046100	Ethylene responsive factor
WCI	Chr16 (1.5–3.4 Mb)	*MdRAV1*	MD16G1047700	Ethylene responsive factor
WCI	Chr13 (2.6–4.4 Mb)	MdMYB62	MD13G1039900	Flavonol biosynthesis
WCI	Chr16 (1.5–3.4 Mb)	MdMYB62	MD16G1040800	Flavonol biosynthesis
IFBD	Chr9 (7.9–11.8 Mb)	MdNAC42	MD09G1147500, MD09G1147600	Anthocyanin accumulation
WCI	Chr17 (11.4–12.4 Mb)	MdNAC42	MD17G1134400	Anthocyanin accumulation
IFBD	Chr9 (7.9–11.8 Mb)	HSP 70	MD09G1137300	Heat stress response
WCI	Chr17 (11.4–12.4 Mb)	HSP 70	MD17G1127600	Heat stress response
IFBD	Chr4 (11.0–13.0 Mb)	MdMYB85	MD04G1080600	Phenylalanine and lignin biosynthesis
WCI	Chr6 (12.1–13.6 Mb)	MdMYB85	MD06G1064300	Phenylalanine and lignin biosynthesis
IFBD	Chr15 (13.2–14.2 Mb)	MdEBF1	MD15G1171800	Ethylene inhibition
WCI	Chr8 (15.2–17.2 Mb)	MdEBF1	MD08G1150200	Ethylene inhibition
IFBD	Chr15 (53.5–54.9 Mb)	MdEIN3	MD15G1441000	Ethylene insensitive 3 protein
WCI	Chr8 (30.3–31.6 Mb)	MdEIN3	MD08G1245800	Ethylene insensitive 3 protein
IFBD	Chr11 (1.7–3.0 Mb)	MdEIN3	MD11G1022400	Ethylene insensitive 3 protein
WCI	Chr7 (4.1–5.6 Mb)	MdEIN3	MD07G1053500, MD07G1053800	Ethylene insensitive 3 protein
IFBD	Chr15 (4.6–6.8 Mb)	MdMYB73	MD15G1076600, MD15G1088000	Cold-stress response & malate accumulation
WCI	Chr15 (24.8–26.8 Mb)	MdMYB73	MD15G1288600	Cold-stress response & malate accumulation
IFBD	Chr15 (4.6–6.8M b)	MdWRKY7	MD15G1078200	Anthocyanin accumulation
WCI	Chr15 (24.8–26.8 Mb)	MdWRKY7	MD15G1287300	Anthocyanin accumulation
IFBD	Chr15 (43.5–45.5 Mb)	MdMYB93	MD15G1369700	Flavonoid & suberin accumulation
WCI	Chr15 (31.7–34.2 Mb)	MdMYB93	MD15G1323500	Flavonoid & suberin accumulation

specific proteases underpinning the WCI-associated regions on Chrs 7 and 15, which is supported by earlier reports suggesting that ubiquitin-specific proteases respond to auxin and might suppress anthocyanin biosynthesis proteins[33]. The auxin

Table 4. List of candidate genes associated with WCI or FBD in the XP-GWA and R6:*MdMYB10* apple datasets.

Mutations in GWAS apple population						Predicted gene function	Expression in R6 and 'Royal Gala' apples		
Gene	Missense SNPs	SNP Stop	Upstream variants	Dataset	Locus	Annotation and TAIR ID	Average RPKM R6 flesh	Average RPKM WT flesh	log2Fold Change
MD02G1132200	1			FBD Supplemental Table S3	Chr02:9450615-11289014	flavanone 3-hydroxylase (F3H, TT6, F3'H) AT3G51240	387	75	2.47
MD02G1133600	3			FBD Supplemental Table S3	Chr02:9450615-11289014	fatty acid desaturase 5 (FAD5) AT3G15850	181	0	9.98
MD02G1153700	1			WCI Table 2	Chr02:11278254-13234556	UDP-Glycosyltransferase, lignin related AT2G18560	1038	534	1.03
MD03G1059200	2			FBD Supplemental Table S3	Chr03:3177994-4910866	Peroxidase AT5G05340	25	1	4.21
MD03G1143300	4		22	FBD Table 1	Chr03:14797661-16611554	bZIP transcription factor (DPBF2, AtbZIP67) AT3G44460	114	852	-2.80
MD03G1147700	12	1		FBD Table 1	Chr03:14797661-16611554	Rho GTPase activating protein AT5G22400	205	89	1.29
MD04G1003400	3		31	WCI Table 2	Chr04:1-1284894	Chalcone synthase (CHS, TT4) AT5G13930	1443	312	2.34
MD04G1204100	6		3	FBD Table 1	Chr04:27629536-29612282	lipoxygenase 1 (LOX1, ATLOX1) AT1G55020	546	268	1.09
MD06G1160700	1		29	FBD Table 1	Chr06:29862341-31737341	peptide met sulfoxide reductase AT4G25130	21212	5456	2.04
MD06G1161400	1		4	FBD Table 1	Chr06:29862341-31737341	Pectin lyase-like protein AT5G63180	6141	29530	-2.22
MD07G1240700	1		26	FBD Supplemental Table S3	Chr07:30357332-31979025	Fe superoxide dismutase 2 AT5G51100	105	1826	-3.99
MD07G1306900			6	FBD Supplemental Table S3	Chr07:34607570-36531467	UDP-glucosyl transferase 78D2 AT5G17050	677	111	2.78
MD08G1249100	2			WCI Supplemental Table S3	Chr08:30486569-31607516	HSP20-like chaperone (ATHSP22.0) AT4G10250	3186	45	6.12
MD09G1114000	3		2	FBD Table 1	Chr09:7999212-11883202	fatty acid desaturase 5 (FAD5) AT3G15850	76	0	8.68
MD09G1146800	1			FBD Table 1	Chr09:7999212-11883202	PHYTOENE SYNTHASE (PSY) AT5G17230	38456	16090	1.32
MD10G1328100	4		5	FBD Supplemental Table S3	Chr10:40235258-41736791	ethylene-forming enzyme (ACO4) AT1G05010	876903	391033	1.21
MD15G1023600	1			FBD Table 1	Chr15:1-1487288	jasmonic acid carboxyl methyltransferase (JMT) AT1G19640	4721	1155	2.07
MD15G1024100			8	FBD Table 1	Chr15:1-1487288	dihydroflavonol 4-reductase (DFR, TT3, M318) AT5G42800	872	309	1.63
MD17G1133400	4			WCI Supplemental Table S3	Chr17:11422073-12433463	PHYTOENE SYNTHASE (PSY) AT5G17230	600	172	1.87
MD17G1260600	2			FBD Supplemental Table S3	Chr17:31098955-32776972	dehydroascorbate reductase 1 (DHAR3) AT5G16710	18	67	−1.78

response factor 9 (*MdARF9*: MD06G1111100), which has also been shown to suppress anthocyanin biosynthesis in RF callus samples[33], also resided in the WCI-associated genomic region on LG7.

Multiple transcription factors play key roles in FBD

Seedlings in both the low- and high-FBD pools carried the *MdMYB10* gene, which suggests that *MdMYB10* itself is not the causal factor of FBD in RF apples. Long-term cold storage generally results in senescence-related flesh breakdown, and several transcription factor genes (e.g. MYB, WRKY, NAC, ERF, cytochrome P450, and HSP) have been shown to express differentially during long-term cold storage[9]. The FBD-associated genomic regions in our study harboured several ERFs, suggesting that ethylene synthesis proteins may be contributing to cell wall disassembly, allowing PPO enzymes to come into contact with phenolic compounds and potentially leading to FBD symptoms[18].

Pectin methyl esterase (PME) genes resided in the FBD-associated significant regions on Chrs 3, 13 and 17. Volatile generation and senescence degradation have been suggested to be bio-markers of FBD, and the expression levels of methyl esters were found to be associated with FBD and senescence in 'Fuji' apples after cold storage[34]. The *MdPME2* gene has also been reported to be associated with apple flesh firmness and mealiness[21,35]. The co-location of genes encoding cell wall-degrading enzymes (*MdPME*) and QTLs for FBD has been reported in apple[18,36].

The clusters of cytochrome P450 enzymes and senescence-related genes resided in some of the FBD-associated regions in

this study. There are no earlier reports of the involvement of P450 enzymes in apple FBD expression, but some genes related to cytochrome P450 were found to be upregulated during litchi fruit senescence[37]. Pericarp browning in litchi is mainly attributable to the degradation of anthocyanin, and the ABA-initiated oxidation of phenolic compounds by PPO[37]. Flavonoids are among the major polyphenols in RF apples[5], and cytochrome P450 is part of the regulatory mechanism for flavonoid metabolism[38]. Association of FBD with the genomic region harbouring P450 would suggest its role in enhanced polyphenol synthesis causing FBD. The co-occurrence of a senescence-related gene MdNAC90 (MD03G1148500; MD11G 11679000) and the PPO regulator germin-like proteins (in the FBD-associated paralog regions on Chrs 3 and 11) lends support to an interplay between senescence and oxidation of phenolics and anthocyanins.

A significant region on Chr9 encompassed a cluster of UGT proteins, which play a role in the regulation of flavonoids and phenolic compounds, as well as converting phloretin to phloridzin[39]. Cytochrome P450, which resided within several FBD-associated regions, is reportedly involved in flavonoid metabolism, such as chlorogenic acid (CGA) acid and phloridzin, which have also been positively associated with suberin production and cell wall disassembly[40,41].

Reactive oxygen species (ROS) play an important role in regulating physiological processes in plants, such as senescence[37]. Legay et al.[42] suggested that *MdMYB93* (MD15G1369700), found residing in the FBD-associated regions in this study, plays a critical role in remobilisation of flavonoid/phenolic compounds, which can be utilised for detoxification of ROS in the case of oxidative stress. However, flavonoid biosynthesis has also been linked with suberin production causing cuticle cracks in apples[42,43], and the development of cuticular cracks could accelerate flesh browning as a result of an enhanced oxidative process[44].

Several HSP (e.g. HSP70, HSP70-1, HSP60, HSP89.1, and HSP DNAJ) and HSF (e.g. HSF4, HSFB4, HSFA6B) resided in the FBD-associated genomic regions. Ferguson et al.[45] showed that, during summer, apple flesh temperature could reach as high as 43 °C, and that an increase in the expression of HSP in apples was associated with high daily flesh temperatures, suggesting a role of HSP to counter heat stress. HSPs have been reported to interact with AP2/ERFs and to play a role in flavonoid biosynthesis and drought tolerance in apple[46]. Heat stress affects lignin accumulation and its substrate, *O*-phenols, and has been reported to play role in enzymatic browning[47]. Additionally, HSF that regulate HSP expression have also been reported to be regulated by cold stress to generate heat-induced cold tolerance in banana[48]. HSF1 was shown to transcriptionally regulate the promoters of HSP to enhance chilling tolerance in loquat fruit[49]. Activity of the enzymes (PAL, C4H, 4CL) of the phenylpropanoid pathway was positively correlated with loquat fruit lignification, whilst suppression of their expression by heat shock treatment and low-temperature conditioning significantly reduced fruit lignification[50].

Wang et al.[7] showed that ascorbate peroxidase (APX) was among the genes that were upregulated in RF apple compared with in white-fleshed apples. Several genes (e.g. *MdAPX1*, *MdAPX3*, *MdAPX4*, and *MdDHAR1*) involved in ascorbate synthesis resided in the genomic regions associated with FBD. Co-localisation of *MdDHAR* and ascorbic acid (AsA) synthesis genes in the FBD-linked genomic regions have been reported[51], suggesting that the low AsA content increases fruit susceptibility to FBD[52]. It has been shown that the expression of *MdMYB1* and *MdDHAR* genes was strongly correlated in RF apples, and that AO and APX were upregulated by anthocyanin regulatory genes[31].

There were several genes associated with CGA biosynthesis residing in the FBD-associated regions on various linkage groups, including the genes MYB19 (MD07G1268000) and *MdC3H* (MD15G1436500). Higher concentrations of CGA were reported in transgenic apple lines carrying *MdMYB10*[12], suggesting a role of CGA metabolism in the expression of FBD[53]. Interestingly, some of the FBD-associated regions (e.g. Chrs 9, 11, 13, 14 and 17) reported here in RF apples coincide with those reported earlier for FBD in white-fleshed apples[18,36,53], suggesting some common underlying genetic mechanisms.

The nexus between WCI and FBD

As discussed above, ERFs have been reported to be involved in the accumulation of anthocyanin and PA biosynthesis, while ethylene synthesis proteins also contribute to cell membrane breakdown, allowing the PPO enzyme to come into contact with phenolic compounds, potentially leading to FBD symptoms[12,18]. We observed clusters of anthocyanin biosynthesis proteins (bHLH), ERFs (*MdERF2*, *MdERF4*, *MdERF12*) and PPO genes together in the genomic region associated with WCI on Chr10. The co-occurrence of these gene families perhaps facilitates potential interactions that contribute to the genetic correlation between WCI and FBD. We noted that genes involved in flavonoid regulation and ethylene synthesis occurred together in the FBD-associated regions on several chromosomes (e.g. MD16G1140800 and *MdPAE10*: MD16G1132100; *MdERF1B*: MD16G1216900 and *MdMYB15*: MD16G1218000, MD16G1218900) – suggesting these genes could be in linkage disequilibrium and this would contribute to the expression of WCI and FBD.

MYB7 (MD16G1029400) resided in the WCI-associated upper region of Chr16, and the expression level of *MYB7* was shown to be correlated with that of *LAR1* in peach fruit[54]. The *MdLAR1* protein (MDP0000376284), which is located about 1.2 Mb upstream of *MYB7* (MD16G1029400), was reported to be associated with WCI and FBD in apple[3]. Mellidou et al.[36] reported that 4CL (MD13G1257800 in the FBD-linked region on Chr13), which catalyses the last step of the phenylpropanoid pathway, leading either to lignin or to flavonoids, was upregulated in browning-affected flesh tissues. The gene *MdMYB85*, involved in the regulation of flavonoid and lignin biosynthesis, resided in the WCI-associated region on Chr6 and FBD-associated paralogous region on Chr4. Metabolic interactions between anthocyanin and lignin biosynthesis have been reported for apple[55] and strawberry[56], while flesh lignification and internal browning during low-temperature storage in a red-fleshed loquat cultivar was shown to be modulated by the interplay between *ERF39* and *MYB8*[57].

The co-localisation of *MdMYB66* and cytochrome P450 proteins, along with the anthocyanin regulatory protein *MdMYB86*, in paralogous FBD-associated genomic regions on Chr6 and Chr14 suggests that these genes interact as a 'hub' contributing to the WCI-FBD genetic link. The paralogs of some other genes were found to be residing in the regions

associated with either WCI or FBD. For example, *MdNAC42* and HSP70 co-localised in the FBD-associated region on Chr9, but this same pair of genes also resided in the most prominent region associated with WCI on Chr17. Similarly, paralogs of *MdEIN3* resided in the WCI-associated region on Chr7 (MD07G1053500, MD07G1053800) and FBD-associated region on Chr11 (MD11G1022400). Interestingly, the paralogs of *MdMYB73* and *MdWRKY7* co-localised in the WCI- (24.6–26.8 Mb) and FBD-associated (4.6–6.8 Mb) regions on Chr15. The WCI-associated region at the bottom of Chr11 hosted a cluster of senescence-related genes, along with the anthocyanin biosynthesis gene *MdbHLH3* (MD11G1286900), suggesting they might interact in the genetic nexus between FBD and WCI.

FBD in RF apples can be caused by senescence, injury via extreme temperature exposure (chilling or heat), or enzymatic (cut fruit) reaction. Genes reported to be connected to all three factors were located in various FBD-associated genomic regions in this study. Postharvest strategies that both delay senescence and limit exposure to low temperatures may be needed to manage FBD. We also hypothesise that high ascorbic acid content could help to minimise expression of FBD in Type-1 RF cultivars. The adverse genetic correlation between WCI and FBD appears to arise from dual and/or interactive roles of several transcription factors, which would pose challenges for designing a conventional marker-assisted selection strategy. The use of bivariate genomic BLUP to estimate breeding values to simultaneously improve adversely correlated polygenic traits (e.g. WCI and FBD), could be an alternative approach[58,59].

MATERIALS AND METHODS

Generation of red-fleshed seedling populations

A population of 900 apple seedlings composed of 24 full-sib families was generated in 2011 by selected crossings between six red-leaved pollen parents and six white-fleshed female parents. All six pollen parents inherited their red-leaf phenotype from the same great-grandparent 'Redfield'[1]. Each pollen parent was involved in four crosses, and the female parents were involved in three to six crosses each. Foliage colour of young seedlings is a phenotypic marker for Type 1 RF apple. The main purpose of this trial was to understand the flesh colour variation and FBD in the Type 1 RF seedlings, so only the seedlings with red foliage (i.e. carrying MdMYB10) were kept for this trial. The number of seedlings per family varied from 10 to 95. The seedlings were grafted onto 'M9' rootstock and were planted in duplicate at the Plant & Food Research orchard in Hawke's Bay, New Zealand (39°39′ S, 176°53′ E) in 2015.

Phenotyping for RF and FBD was conducted over two consecutive fruiting seasons (2017 and 2018). Fruit were harvested once, when judged mature, based on a change in skin background colour from green to yellow, and when the starch pattern index (SPI) was between 1.0 and 2.0 (on a scale of 0 to 7). In each season, six fruit were harvested from each plant and stored for 70 d at 0.5 °C, followed by 7 d at 20 °C before fruit evaluation. Fruit were cut in half across the equator and the proportion of the cortex area (PRA) that was red in colour, and the intensity of the red colour (RI) (= 1 (low) to 9 (high)) was scored. A weighted cortical intensity (WCI) was then calculated (PRA × RI) as an estimation of the amount of red pigment in the fruit. The proportion of the cortex area showing symptoms of FBD was also recorded. WCI and FBD were averaged over all fruit for a particular seedling. Fruit were also assessed for the following eating quality traits on a 1 (lowest) to 9 (highest) scale: firmness, crispness, juiciness, sweetness, sourness and astringency, to understand the genetic correlations of eating-quality traits with WCI and FBD.

Generation of R6:*MdMYB10* apple fruit

The binary vector pSA277-R6:MYB10 was transferred into *Agrobacterium tumefaciens* strain LAB4404 by electroporation. Transgenic 'Royal Gala' plants were generated by *Agrobacterium*-mediated transformation of leaf pieces, using a method previously reported[5]. Wild-type 'Royal Gala' and three independent transgenic lines (A2, A4 and A10) of *R6:MdMYB10* were grown under glasshouse conditions in full potting mix with natural light. The resulting fruit were assessed for flesh colour phenotypes at harvest (around 135 d after full bloom). Fruit peel and cortex from three biological replicates were collected and frozen in liquid nitrogen, with each replicate compiled from five pooled mature fruit for each transgenic line or wild-type control.

Real-Time quantitative RT-qPCR analysis

Total RNA of 36 samples (3 *R6:MYB10* lines and 1 wild type control, 3 time points, 3 biological replicates) was extracted, using Spectrum Plant Total RNA Kit (SIGMA). Removal of genomic DNA contamination and first-strand cDNA synthesis were carried out using the mixture of oligo (dT) and random primers according to the manufacturer's instructions (QuantiTect Reverse Transcription Kit, Qiagen). Real-time qPCR DNA amplification and analysis was carried out using the LightCycler 480 Real-Time PCR System (Roche), with LightCycler 480 software version 1.5. The LightCycler 480 SYBR Green I Master Mix (Roche) was used following the manufacturer's method. The qPCR conditions were 5 min at 95 °C, followed by 45 cycles of 5 s at 95 °C, 5 s at 60°C, and 10 s at 72 °C, followed by 65 °C to 95 °C melting curve detection. The qPCR efficiency of each gene was obtained by analyzing the standard curve of a cDNA serial dilution of that gene. The expression was normalized to *Malus* × *domestica* elongation factor 1-alpha *MdEF1α* (XM_008367439) due to its consistent transcript levels throughout samples, with crossing threshold values changing by less than 2.

Phenotypic data analysis

Individual fruit measurements were first averaged for each seedling. As the phenotyping was repeated over two years, we used a mixed linear model (MLM) accounting for this 'permanent environmental effect', as previously described[58]. Pedigree-based additive genetic relationships among seedlings were taken into account for estimation of genetic parameters using ASReml software[60]. Product-moment correlations between best linear unbiased predictions (BLUP) of breeding values of all seedlings for different traits were used as estimates of genetic correlation among traits.

Identification of extreme phenotypes, pool-sequencing, and QC of sequence data

A selective DNA pooling procedure was adopted to construct DNA pools. A high-pool and a low-pool were constructed separately for the two traits (WCI and FBD). Genomic DNA was extracted from the leaves of selected seedlings, and quantified by fluorimetry using the picogreen reagent (Cat#P11496, Thermo). The low and high pools consisted of 35 seedlings

each, and normalised amounts (~300 ng) of DNA from individuals were pooled. The pools were dried down with DNA Stable reagent (Cat#93021001, Biomatrica) in a centrifugal evaporator and shipped for sequencing. Each DNA pool was sequenced using paired-end 125 bp reads on the Illumina HiSeq 2500 platform. The quality of raw sequence reads was checked with FastQC/0.11.2 and MultiQC/1.2. Based on the quality control reports, the reads were aligned to the published apple reference genome GDDH13 v1.1[61] using the program bowtie2/2.3.4.3[62] with trimming from both ends before alignments and aligning in full read length ("-5 6 -3 5 –end-to-end"). The mapping results were marked for duplicate alignments, sorted, compressed and indexed with samtools/1.12[63]. Based on the alignment of binary alignment map (BAM) files of the high and low pools, single nucleotide polymorphism (SNP) identification was performed using samtools/1.12 ('samtools mpileup') and bcftools/1.12 ('bcftools call –mv')[63,64]. Variant sites with missing genotype in any of the pools, or having the same genotype between the pools, were discarded. To minimise the influence of sequencing quality on association analysis, the identified SNPs were further filtered according to the following criteria: 1) a Phred-scaled quality score > 20; and 2) the read depth in each pool was neither < 35, nor > 500.

Association test using DNA pools

The allele frequencies between each pair of bulk DNAs (low versus high WCI; low versus high FBD) were compared at each SNP locus. Differences in the allele frequencies between the low and high pool were expected to be negligible for unlinked SNP markers, but allele frequency differences would be larger for SNPs closely linked to the underlying quantitative trait loci (QTLs) contributing to the extreme phenotypes. A nonparametric test (G-statistic = $2 \times \Sigma n_i \ln(n_i/n_{exp})$, where n_i (i = 1 to 4) represented counts of reference and alternate alleles at a particular SNP generated from sequencing of the low and high pool, and n_{exp} was the expected allele count assuming no allele frequency divergence between the two DNA pools[65].

We then calculated a modified statistic (G'), which took into account read count variation caused by sampling of segregants as well as variability inherent in short-read sequencing of pooled samples[65]. Using R package QTLseqr[66], firstly a G-statistic was calculated for each SNP marker, and then a weighted average using Nadaraya-Watson kernel was obtained to yield a G' statistic for a sliding genomic window of 2 Mb size. The Nadaraya-Watson method weights neighbouring markers' G-values by their distance from the focal SNP so that closer SNPs receive higher weights. The 95th percentile value of G' was used as a threshold to identify significant hotspots and to identify the putative candidate genes residing within the ±1 Mb region around the G' peak. For comparison purposes, a standard two-sided Z-test[14] was also performed to determine the significance of allele frequency differences at SNP loci between the pools for each trait.

Candidate gene identification

The GDDH gene models intersecting with the XP-GWA hotspots were pulled out with bedtools/2.30.0 ("bedtools intersect -wo -nonamecheck"). The selected genes were further blasted to TAIR10 ("-evalue 1e-5") and the annotated functions from Arabidopsis genes with the best blast score, the highest % identity, and the longest aligned length, were used. Then the expressions of genes located in the GWA hotspots were extracted from the RNAseq analysis of the R6:*MdMYB10* representative transgenic line, and the log 2-fold change between the *R6:MdMYB10* and 'Royal Gala' apples were calculated.

ACKNOWLEDGMENTS

This research was funded in 2017/18 by the Strategic Science Investment Fund of the New Zealand Ministry of Business, Innovation and Employment (MBIE) and from 2019 by the Plant & Food Research Technology Development – Pipfruit programme. We thank our colleague Jason Johnston for providing some pictures of the flesh browning disorder in red-fleshed apples. Richard Volz and Jason Johnston provided constructive comments and suggestions on the manuscript.

Conflict of interest

The authors declare that they have no conflict of interest.

Supplementary Information accompanies this paper at (https://www.maxapress.com/article/doi/10.48130/FruRes-2022-0012)

Dates

Received 20 May 2022; Accepted 12 August 2022; Published online 29 August 2022

REFERENCES

1. Volz RK, Oraguzie N, Whitworth C, How N, Chagne D. et al. 2009. Breeding for red flesh colour in apple: progress and challenges. *Acta Horticulturae* 814:337–42
2. Espley RV, Hellens RP, Putterill J, Stevenson DE, Kutty-Amma S, et al. 2007. Red colouration in apple fruit is due to the activity of the MYB transcription factor, MdMYB10. *The Plant Journal* 49:414–27
3. Kumar S, Garrick DJ, Bink MC, Whitworth C, Chagné D, et al. 2013. Novel genomic approaches unravel genetic architecture of complex traits in apple. *BMC Genomics* 14:393
4. Volz RK, Kumar S, Chagné D, Espley R, McGhie TK, et al. 2013. Genetic relationships between red flesh and fruit quality traits in apple. *Acta Horticulyurae* 976:363–68
5. Espley RV, Brendolise C, Chagne D, Kutty-Amma S, Green S, et al. 2009. Multiple repeats of a promoter segment causes transcription factor autoregulation in red apples. *The Plant Cell* 21:168–83
6. van Nocker S, Berry G, Najdowski J, Michelutti R, Luffman M, et al. 2012. Genetic diversity of red-fleshed apples (*Malus*). *Euphytica* 185:281–93
7. Wang N, Zheng Y, Duan N, Zhang Z, Ji X, et al. 2015. Comparative transcriptomes analysis of red-and white-fleshed apples in an F1 population of *Malus sieversii f. niedzwetzkyana* crossed with *M. domestica* 'Fuji'. *PLoS One* 10:e0133468
8. Zhang S, Chen Y, Zhao L, Li C, Yu J, et al. 2020. A novel NAC transcription factor, *MdNAC42*, regulates anthocyanin accumulation in red-fleshed apple by interacting with *MdMYB10*. *Tree physiology* 40:413–23
9. Zhao J, Quan P, Liu H, Li L, Qi S, et al. 2020. Transcriptomic and metabolic analyses provide new insights into the apple fruit quality decline during long-term cold storage. *Journal of Agricultural and Food Chemistry* 68:4699–716
10. Zhang J, Xu H, Wang N, Jiang S, Fang H, et al. 2018. The ethylene response factor MdERF1B regulates anthocyanin and proanthocyanidin biosynthesis in apple. *Plant Molecular Biology* 98:205–18

11. Li H, Han M, Yu L, Wang S, Zhang J, et al. 2020a. Transcriptome analysis identifies two ethylene response factors that regulate proanthocyanidin biosynthesis during *Malus crabapple* fruit development. *Frontiers in Plant Science* 26:76
12. Espley RV, Leif D, Plunkett B, McGhie T, Henry-Kirk R, et al. 2019. Red to brown: an elevated anthocyanic response in apple drives ethylene to advance maturity and fruit flesh browning. *Frontiers in Plant Science* 10:1248
13. Zuo W, Lu L, Su M, Zhang J, Li Y, et al. 2021. Analysis of differentially expressed genes and differentially abundant metabolites associated with the browning of Meihong red-fleshed apple fruit. *Postharvest Biology and Technology* 174:111437
14. Huang W, Kirkpatrick BW, Rosa GJ, Khatib H. 2010. A genome-wide association study using selective DNA pooling identifies candidate markers for fertility in Holstein cattle. *Animal Genetics* 41:570–78
15. Yang J, Jiang H, Yeh CT, Yu J, Jeddeloh JA, et al. 2015. Extreme-phenotype genome-wide association study (XP-GWAS): a method for identifying trait-associated variants by sequencing pools of individuals selected from a diversity panel. *The Plant Journal* 84:587–96
16. Zheng W, Shen F, Wang W, Wu B, Wang X, et al. 2020. Quantitative trait loci-based genomics-assisted prediction for the degree of apple fruit cover color. *The Plant Genome* 13:e20047
17. Zhang S, Yang J, Li H, Chiang VL, Fu Y. 2021. Cooperative regulation of flavonoid and lignin biosynthesis in plants. *Critical Reviews in Plant Sciences* 27:109–26
18. Di Guardo M, Tadiello A, Farneti B, Lorenz G, Masuero D, et al. 2013. A multidisciplinary approach providing new insight into fruit flesh browning physiology in apple (*Malus* × *domestica* Borkh.). *PLoS One* 18:e78004
19. Sun Q, Jiang S, Zhang T, Xu H, Fang H, et al. 2019. Apple NAC transcription factor *MdNAC52* regulates biosynthesis of anthocyanin and proanthocyanidin through *MdMYB9* and *MdMYB11*. *Plant Science* 289:110286
20. Urrestarazu VJ, Muranty H, Denancé C, Leforestier D, Ravon E, et al. 2017. Genome-wide association mapping of flowering and ripening periods in apple. *Frontiers in Plant Science* 8:1923
21. Wu B, Shen F, Chen C, Liu L, Wang X, et al. 2021a. Natural variations in a pectin acetylesterase gene, *MdPAE10*, contribute to prolonged apple fruit shelf life. *The Plant Genome* 14:e20084
22. Hu D, Li Y, Zhang Q, Li M, Sun C, et al. 2017. The R2R3-MYB transcription factor MdMYB 73 is involved in malate accumulation and vacuolar acidification in apple. *The Plant Journal* 91:443–54
23. Zhang Q, Yu J, Wang J, Hu D, Hao Y. 2017. Functional characterization of *MdMYB73* reveals its involvement in cold stress response in apple calli and Arabidopsis. *Journal of Integrative Agriculture* 16:2215–21
24. Wu B, Shen F, Wang X, Zheng W, Xiao C, et al. 2021b. Role of *MdERF3* and *MdERF118* natural variations in apple flesh firmness/crispness retainability and development of QTL-based genomics-assisted prediction. *Plant Biotechnology Journal* 19:1022–37
25. Li H, Li Y, Yu J, Wu T, Zhang J, et al. 2020b. *MdMYB8* is associated with flavonol biosynthesis via the activation of the *MdFLS* promoter in the fruits of *Malus crabapple*. *Horticulture Research* 7:19
26. Geng D, Shen X, Xie Y, Yang Y, Bian R, et al. 2020. Regulation of phenylpropanoid biosynthesis by MdMYB88 and MdMYB124 contributes to pathogen and drought resistance in apple. *Horticulture Research* 7:102
27. Xie Y, Bao C, Chen P, Cao F, Liu X, et al. 2021. Abscisic acid homeostasis is mediated by feedback regulation of *MdMYB88* and *MdMYB124*. *Journal of Experimental Botany* 72:592–607
28. Chen Z, Yu L, Liu W, Zhang J, Wang N, et al. 2021. Research progress of fruit color development in apple (*Malus domestica* Borkh.). *Plant Physiology and Biochemistry* 162:267–79
29. Wu R, Wang Y, Wu T, Xu X, Han Z. 2017. *MdMYB4*, an R2R3-Type MYB transcription factor, plays a crucial role in cold and salt stress in apple calli. *Journal of the American Society for Horticultural Science* 142:209–16
30. An J, Wang X, Li Y, Song L, Zhao L, et al. 2018. EIN3-LIKE1, MYB1, and ETHYLENE RESPONSE FACTOR3 act in a regulatory loop that synergistically modulates ethylene biosynthesis and anthocyanin accumulation. *Plant Physiology* 178:808–23
31. An J, Zhang X, Bi S, You C, Wang X, et al. 2020. The ERF transcription factor MdERF38 promotes drought stress-induced anthocyanin biosynthesis in apple. *The Plant Journal* 101:573–89
32. Lu Y, Bu Y, Hao S, Wang Y, Zhang J, et al. 2017. MYBs affect the variation in the ratio of anthocyanin and flavanol in fruit peel and flesh in response to shade. *Journal of Photochemistry and Photobiology B: Biology* 168:40–49
33. Ji XH, Zhang R, Wang N, Yang L, Chen XS. 2015. Transcriptome profiling reveals auxin suppressed anthocyanin biosynthesis in red-fleshed apple callus (*Malus sieversii* f. niedzwetzkyana). *Plant Cell, Tissue and Organ Culture* 123:389–404
34. Tanaka F, Tatsuki M, Matsubara K, Okazaki K, Yoshimura M, et al. 2018. Methyl ester generation associated with flesh browning in 'Fuji'apples after long storage under repressed ethylene function. *Postharvest Biology and Technology* 145:53–60
35. Segonne SM, Bruneau M, Celton JM, Gall SL, Francin-Allami M, et al. 2014. Multiscale investigation of mealiness in apple: an atypical role for a pectin methylesterase during fruit maturation. *BMC Plant Biology* 14:375
36. Mellidou I, Buts K, Hatoum D, Ho QT, Johnston JW, et al. 2014. Transcriptomic events associated with internal browning of apple during postharvest storage. *BMC Plant Biology* 14:328
37. Yun Z, Qu H, Wang H, Zhu F, Zhang Z, et al. 2016. Comparative transcriptome and metabolome provides new insights into the regulatory mechanisms of accelerated senescence in litchi fruit after cold storage. *Scientific Reports* 6:19356
38. Ayabe SI, Akashi T. 2006. Cytochrome P450s in flavonoid metabolism. *Phytochemistry Reviews* 5:271–82
39. Zhou K, Hu L, Li P, Gong X, Ma F. 2017. Genome-wide identification of glycosyltransferases converting phloretin to phloridzin in *Malus* species. *Plant Science* 265:131–45
40. Valiñas MA, Lanteri ML, ten Have A, Andreu AB. 2015. Chlorogenic acid biosynthesis appears linked with suberin production in potato tuber (*Solanum tuberosum*). *Journal of Agricultural and Food Chemistry* 63:4902–13
41. Gutierrez BL, Zhong G, Brown SK. 2018. Increased phloridzin content associated with russeting in apple (*Malus domestica* (Suckow) Borkh.) fruit. *Genetic Resources and Crop Evolution* 65:2135–49
42. Legay S, Guerriero G, André C, Guignard C, Cocco E, et al. 2016. *MdMYB93* is a regulator of suberin deposition in russeted apple fruit skins. *New Phytologist* 212:977–91
43. Joshi M, Baghel RS, Fogelman E, Stern RA, Ginzberg I. 2018. Identification of candidate genes mediating apple fruit-cracking resistance following the application of gibberellic acids 4 + 7 and the cytokinin 6-benzyladenine. *Plant Physiology and Biochemistry* 127:436–445
44. Lara I, Belge B, Goulao LF. 2014. The fruit cuticle as a modulator of postharvest quality. *Postharvest Biology and Technology* 87:103–12
45. Ferguson IB, Snelgar W, Lay-Yee M, Watkins CB, Bowen JH. 1998. Expression of heat shock protein genes in apple fruit in the field. *Functional Plant Biology* 25:155–63
46. Wang N, Liu W, Yu L, Guo Z, Chen Z, et al. 2020. Heat shock factor A8a modulates flavonoid synthesis and drought tolerance. *Plant Physiology* 184:1273–90
47. Racsko J, Schrader LE. 2012. Sunburn of apple fruit: Historical background, recent advances and future perspectives. *Critical Reviews in Plant Sciences* 31:455–504

48. Wei Y, Hu W, Xia F, Zeng H, Li X, et al. 2016. Heat shock transcription factors in banana: genome-wide characterization and expression profile analysis during development and stress response. *Scientific Reports* 6:36864
49. Zeng JK, Li X, Zhang J, Ge H, Yin XR, et al. 2016. Regulation of loquat fruit low temperature response and lignification involves interaction of heat shock factors and genes associated with lignin biosynthesis. *Plant Cell Environment* 39:1780–1789
50. Li X, Zang C, Ge H, Zhang J, Grierson D, et al. 2017. Involvement of PAL, C4H, and 4CL in chilling injury-induced flesh lignification of loquat fruit. *HortScience* 52:127–31
51. Mellidou I, Chagné D, Laing WA, Keulemans J, Davey MW. 2012. Allelic variation in paralogs of GDP-L-galactose phosphorylase is a major determinant of vitamin C concentrations in apple fruit. *Plant Physiology* 160:1613–29
52. Davey MW, Kenis K, Keulemans J. 2006. Genetic control of fruit vitamin C contents. *Plant Physiology* 142:343–51
53. Kunihisa M, Hayashi T, Hatsuyama Y, Fukasawa-Akada T, Uenishi H, et al. 2021. Genome-wide association study for apple flesh browning: detection, validation, and physiological roles of QTLs. *Tree Genetics & Genomes* 17:11
54. Zhou H, Lin-Wang K, Liao L, Gu C, Lu Z, et al. 2015. Peach MYB7 activates transcription of the proanthocyanidin pathway gene encoding leucoanthocyanidin reductase, but not anthocyanidin reductase. *Frontiers in Plant Science* 6:908
55. Hu Y, Cheng H, Zhang Y, Zhang J, Niu S, et al. 2021. The MdMYB16/MdMYB1-miR7125-MdCCR module regulates the homeostasis between anthocyanin and lignin biosynthesis during light induction in apple. *New Phytologist* 231:1105–22
56. Ring L, Yeh SY, Hücherig S, Hoffmann T, Blanco-Portales R, et al. 2013. Metabolic interaction between anthocyanin and lignin biosynthesis is associated with peroxidase *FaPRX27* in strawberry fruit. *Plant Physiology* 163:43–60
57. Zhang J, Yin X, Li H, Xu M, Zhang M, et al. 2020. ETHYLENE RESPONSE FACTOR39 – MYB8 complex regulates low-temperature-induced lignification of loquat fruit. *Journal of Experimental Botany* 71:3172–84
58. Kumar S, Chagné D, Bink MCAM, Volz RK, Whitworth C, et al. 2012. Genomic selection for fruit quality traits in apple (*Malus* × *domestica* Borkh.). *PLoS One* 7:e36674
59. Strandén I, Kantanen J, Russo IRM, Orozco-terWengel P, Bruford MW. 2019. Genomic selection strategies for breeding adaptation and production in dairy cattle under climate change. *Heredity* 123:307–17
60. Gilmour AR, Cullis BR, Harding SA, Thompson R. 2006. *ASReml Update: what's new in Release 2.00*. VSN Int. Ltd, Hemel Hempstead, UK.
61. Daccord N, Celton JM, Linsmith G, Becker C, Choisne N, et al. 2017. High-quality *de novo* assembly of the apple genome and methylome dynamics of early fruit development. *Nature Genetics* 49:1099–106
62. Langmead B, Salzberg SL. 2012. Fast gapped-read alignment with Bowtie 2. *Nature Methods* 9:357–59
63. Li H. 2011. A statistical framework for SNP calling, mutation discovery, association mapping and population genetical parameter estimation from sequencing data. *Bioinformatics* 27:2987–93
64. Danecek P, Bonfield JK, Liddle J, Marshall J, Ohan V, et al. 2021. Twelve years of SAMtools and BCFtools. *GigaScience* 10:giab008
65. Magwene PM, Willis JH, Kelly JK. 2011. The statistics of bulk segregant analysis using next generation sequencing. *PLoS Computational Biology* 7:e1002255
66. Mansfeld BN, Grumet R. 2018. QTLseqr: an R package for bulk segregant analysis with next-generation sequencing. *The Plant Genome* 11:180006